The usefulness of near-field goniophotometry data to assess illuminances and discomfort glare in indoor lighting

Lionel Simonot, Frédéric Reux, Samuel Carré, Christophe Martinsons

The usefulness of near-field goniophotometry data to assess illuminances and discomfort glare in indoor lighting

L. Simonot[a]*, F. Reux[b], S. Carré[c] and C. Martinsons[d]

[a]Université de Poitiers, Institut Pprime UPR 3346 CNRS, Chasseneuil Futuroscope, France, [b]Université de Poitiers, ENSI Poitiers, France, [c]Centre Scientifique et Technique du Bâtiment, Nantes, France, [d]Centre Scientifique et Technique du Bâtiment, Saint Martin d'Hères, France,

*corresponding author: lionel.simonot@univ-poitiers.fr

Orcid

Lionel Simonot http://orcid.org/0000-0002-3497-2647

Samuel Carré http://orcid.org/0000-0002-0484-2331

Christophe Martinsons http://orcid.org/0000-0002-2286-5991

The usefulness of near-field goniophotometry data to assess illuminances and discomfort glare in indoor lighting

In lighting simulations, a luminaire is usually modeled using a luminous intensity distribution emitted by a single point source. This so-called far-field approach is valid as long as the dimensions of the luminaire are much smaller than the distance to the calculation surface. This assumption is generally not met in standard indoor lighting and may lead to significant errors in the prediction of illuminances and discomfort glare. This work describes a practical near-field approach based on splitting the luminaire into *N* point sources. The errors in relation to the near field (infinite value of *N*) are evaluated as a function of *N*. This approach generates a more accurate assessment of the Unified Glare Rating in the case of luminaires with non-uniform emission.

Keywords: discomfort glare; near-field goniophotometry; indoor lighting; lighting simulation; photometry

1. Introduction

Simulations for lighting design very often consider light sources as point sources. Each luminaire is generally defined by a photometric data file, such as an IES file, which contains the intensity angular distribution, applied at the center of the luminaire. This strong assumption is a far-field approximation requiring the largest luminaire dimension to be much smaller than the distance between the luminaire and the calculation surface. For decades, it has been estimated that a ratio of 5 between these dimensions makes it possible to apply this approximation satisfactorily. In street and road lighting, where fairly compact luminaires are placed several meters above the ground, the far-field approximation gives acceptable results in most practical cases. This is not true in the case of many architectural lighting designs, using for instance, wall-washing luminaires.

For indoor lighting simulations, the use of far-field goniophotometry should be questioned. Indeed, recessed ceiling luminaires with dimensions 600 x 600 mm^2 are

among the most widely used. Even in the most standard configurations, it is difficult to reduce these luminaires to a single point. Firstly, the maximal size of the luminaires (~0.84 m for the diagonal) is not negligible compared with the distance from the calculation plane (typically between 1.4 m and 2 m). Secondly, this simplification cannot describe the effects of the spatial non-uniformity of the luminance across the emitting surface.

Near-field goniophotometry data can be used to overcome these limitations by describing the luminance angular distribution at each point of the luminaire. In the 1990s, Ian Ashdown revisited the basics of near-field goniophotometry for lighting (Ashdown 1993). His approach has made it possible to define a new family of goniophotometers (Ashdown 1998). These near-field goniophotometers rely on the use of a calibrated imaging system to record luminance images of the luminaire in all directions (Boulenguez 2008). Compared to their far-field equivalent, these devices have the advantage of being more compact. They do not require a long distance between the luminaire and the photodetector. The cost of near-field goniophotometers is generally lower than far-field instruments, which explains the development of commercial systems in recent years. Most near-field goniophotometers software convert the luminance images into far-field intensity distribution curves adapted to lighting simulation software, the vast majority of which being based on far-field photometric calculations. Taking into account the luminance spatial distribution of extended light sources would significantly increase calculation times. But current computing powers would allow these more accurate simulations to be performed in many practical configurations. Nevertheless, this feature has not been offered yet to lighting professionals, probably because of the belief that near-field calculations would only bring negligible corrections, without any consequence in

usual lighting criteria based on the illuminance distribution and the Unified Glare Rating (UGR) for instance.

In the literature, some authors (Holmes 1990, Stannard 1990, Ngai 1993) propose to apply the far-field calculations by replacing the luminous intensity distribution by a "working" intensity measured at a distance corresponding to the usage situation. However, this approach is difficult to generalize because it would require luminaire manufacturers to provide as many working luminous intensity distributions as the number of possible configurations. Another approach (Lautzenheiser 1984, Ngai 1987) is to use near-field goniophotometry data to split the luminaire into N small point sources. It is then possible to model a luminaire by N point sources in a lighting simulation software. The value of N is used to adjust the level of accuracy in the near-field description of the luminaire. The most frequently used lighting simulation software (DIALux evo, ReluxDesktop, AGI32) offer this option more or less explicitly. The choice of the number N is for example limited. These software spatially distribute the far-field luminous intensity distribution on the surface of the luminaire. This approach is justified in the case of a uniform emission but not for non-uniform ones.

In this paper, we adopt this approach of dividing the luminaire surface area by discussing in more detail its impact on the evaluation of illuminances and UGR. In Section 2, photometric quantities are defined with far-field and near-field approaches. We present the procedure consisting in dividing the luminaire into N surfaces and study the influence of N in the case of a luminaire with uniform and Lambertian emission. In Section 3, we apply this approach to a standard interior lighting configuration. We consider an LED panel luminaire with a diffuser whose emission is assumed to be uniform, and a luminaire fitted with fluorescent tubes whose emission is non-uniform. In Section 4, we discuss the evaluation of the UGR for a luminaire with a non-uniform emission using the recent CIE

technical report (CIE 232:2019). In the conclusion of this paper, we discuss about implementing this method in order to control the uncertainty in the illuminance and UGR values in the case of indoor lighting extended luminaires.

2. Near-field vs far-field for surface luminaire

Typical level of uncertainty in photometric measurements

In this study, we are comparing methods for calculating photometric quantities. It is therefore important to first define the uncertainties that can be expected from a photometric measurement in order to justify or not the use of more complex calculations. All photometric quantities are defined by the candela, one of the seven units of the international system. Each of these fundamental units is defined in relation to a constant. For the candela, this is the luminous efficiency at 555 nm of the standard observer defined by the CIE, $K_m = 683$ lm/W . The CIE technical report 198:2011 details the process of estimating uncertainties in photometric measurements. Without being exhaustive, we can mention several sources of uncertainties that combine together: measurement distance error, angular alignment error, temperature drift, calibration uncertainties, spectral mismatch error, linearity error, etc. Even without knowing each of these sources of uncertainty, a photometric quantity can be expected to be measured with a combined uncertainty of 2% or 1 % at the very best. The corollary is that there is no need for more complex and time-consuming photometric calculations if the objective is to achieve a numerical accuracy of about 1%. It should also be noted that accuracies of up to 10% are acceptable for most applications (DiLaura 2011).

A significant source of uncertainty comes from interpolations of the luminous intensity distributions, especially if the angular sampling is coarse and/or if the intensity distribution presents sharp variations. Nevertheless, we will assume thereafter that this

source of uncertainty is negligible in order to focus our study on the consideration of the surface aspect of the sources (non-uniformity of the luminous intensity distribution across the emitting surface).

Luminance and luminous intensity

For each light-emitting point, a direction is defined by the zenithal γ and azimuthal C angles related to the photometric spherical system centered on this point and having as its axis the normal to the emitting surface. We consider a surface source with a (u,v) spatial coordinate system. At each point of the luminaire with coordinates (u,v), we define the luminance $L(u,v,C_{uv},\gamma_{uv})$ emitted in every direction (C_{uv},γ_{uv}). For simplicity, the emission surface is considered to be flat and horizontal so that the direction (C,γ) can be defined relative to the vertical pointing downwards for all points on the source (Fig. 1.a). The luminous intensity distribution $I(C,\gamma)$ can be deduced by the surface integration of the luminance as:

$$I(C,\gamma)=\iint_{u,v} L(u,v,C,\gamma)\cos\gamma\,du\,dv \qquad (1)$$

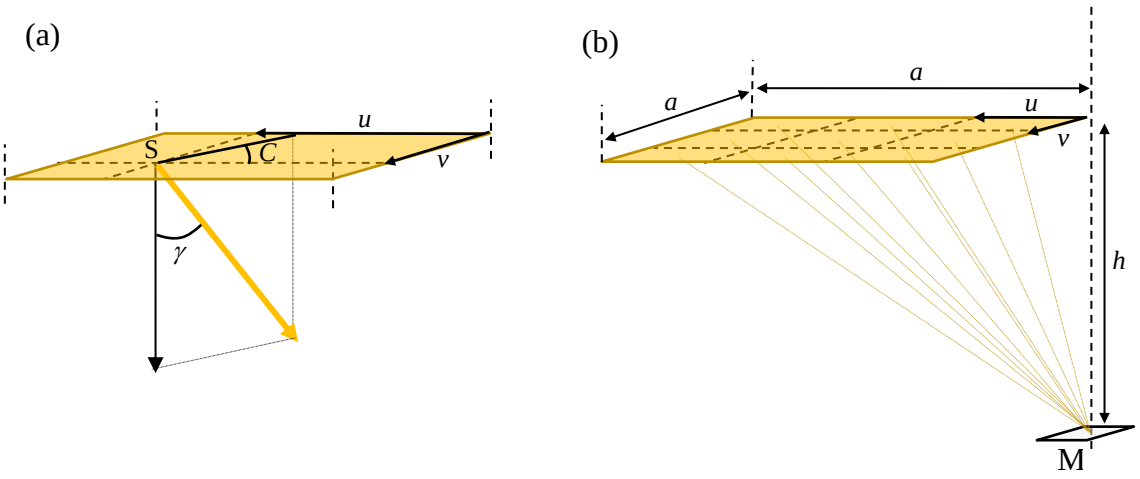

Figure 1. (a) Spatial (u,v) and angular (C,γ) parameters from a point S of an emitting surface. (b) Square luminaire divided in N = 9 small emitting surfaces contributing to the illuminance at point M.

Equation (1) can be discretized by dividing the luminaire into N surfaces centered in (u_i,v_j) and of apparent area $\cos\gamma\Delta u_i\Delta v_j$ from the direction (C,γ):

$$I_N(C,\gamma)=\sum_i\sum_j \bar{L}(u_i,v_j,C,\gamma)\cos\gamma\Delta u_i\Delta v_j \qquad (2)$$

where $\bar{L}(u_i,v_j,C,\gamma)$ is the average luminance over the elementary emitting surface centered in (u_i,v_j).

Equation (2) is equivalent to equation (1) when N tends towards infinity (near-field). Conversely, the case $N=1$ corresponds to the far-field assumption. In this case, the intensity is equal to the average luminance times the apparent surface of the light source in the considered direction.

UGR

In indoor lighting, the discomfort glare can be evaluated with the Unified Glare Rating given by the following equation (CIE Technical report 117:1995):

$$UGR = 8\log\frac{0.25}{L_b}\sum\frac{L^2\omega}{p^2} \quad (3)$$

where L_b is the background luminance, and for each luminaire, L is the average luminance, ω corresponds to the solid angle from which the luminaire is seen by the observer, and p is the Guth index, which depends on the position of the luminaire in relation to the observer's assumed direct horizontal view. The UGR depends on the dimensions of the room, the reflection coefficients of the various surfaces, the arrangement of the luminaires and the position of the observer. Manufacturers give simulated UGR values for standard configurations and for the most penalizing observer position, i.e. at the back of the room.

To obtain the average luminance of the luminaires in a given direction, near-field goniophotometry data would be particularly suitable. Most of the time, luminance is simply deduced from the luminous intensity by dividing by the apparent area of the luminaire seen by the observer. If the luminance is uniform over the entire surface of the luminaire, dividing the luminaire into small emitting surfaces should have no impact on the calculated UGR value. This is because the Guth index varies very little between two points of the same luminaire, and the sum of the solid angles into which the observer sees these different surfaces is equal to the total solid angle at which she or he sees the whole luminaire. Conversely, the calculated UGR values can be very different when the emitting surface has a high luminance contrast. The case of UGR calculations for surface luminaires that are non-uniform in luminance is discussed in Section 4.

Illuminance

In far-field goniophotometry, the illuminance at a point M provided by a point source S is deduced from the intensity $I_{S\to M}$ emitted by the source in the considered direction.

$$E(M)=\frac{I_{S\to M}}{SM^2}\cos\gamma_{M/S} \tag{4}$$

where $\cos\gamma_{M/S}$ is the obliquity factor of the illuminated surface around point M seen from source S.

In the case of the near field, the illuminance at a point M provided by a surface source can be obtained by the surface integration of the luminance $L_{S\to M}$:

$$E(M)=\iint_{u,v}\frac{L_{S\to M}\cos\gamma_{S/M}}{SM^2}\cos\gamma_{M/S}\,du\,dv \tag{5}$$

where (u,v) are the integration parameters and the coordinates of the point S on the luminaire, and $\cos\gamma_{S/M}$ is the obliquity factor of the emitting surface around point *S* seen from point M.

Similar to equation (2), it is possible to divide the luminaire into *N* smaller areas. In this way, the equation (5) is discretized as:

$$E_N(M)=\sum_i\sum_j\frac{\overline{L}_{S_{ij}\to M}\cos\gamma_{S_{ij}/M}}{S_{ij}M^2}\cos\gamma_{M/S_{ij}}\Delta u_i\Delta v_j \tag{6}$$

where $\overline{L}_{S_{ij}\to M}$ is the average luminance over the elementary emitting surface centered in $S_{ij}(u_i,v_j)$ and towards point M.

Figure 1.b illustrates the calculation principle for N = 9. Equation (6) can be written as a function of the intensity $I_{S_{ij}\to M} = \bar{L}_{S_{ij}\to M} \cos\gamma_{S_{ij}/M} \Delta u_i \Delta v_j$ of each elementary emitting surface around point S_{ij} and towards point M:

$$E_N(M) = \sum_i \sum_j \frac{I_{S_{ij}\to M}}{S_{ij}M^2} \cos\gamma_{M/S_{ij}} \tag{7}$$

Equations (6) and (7) are equivalent to equation (5) (near-field) when N tends towards infinity and to equation (4) (far-field) when N = 1.

Case study of a uniform Lambertian luminaire

In the following sections, we consider flat and square recessed ceiling luminaires of side a = 0.6 m. We consider the illuminance on a horizontal plane. The luminaire is divided into N small surfaces of area a^2/N (see Fig. 1.b for N = 9). Under these assumptions, $cos\,\gamma_{S_{ij}/M} = cos\,\gamma_{M/S_{ij}} = \frac{h}{S_{ij}M}$ and Eq. (6) becomes:

$$E_N(M) = \frac{a^2}{N} \sum_i \sum_j \bar{L}_{S_{ij}\to M} \frac{h^2}{S_{ij}M^4} \tag{8}$$

where h is the height between the illuminance calculation surface and the ceiling.

We now consider the luminaire to be uniform in luminance and Lambertian, i.e. it emits a constant luminance throughout the lower hemisphere. This is probably one of the configurations where the difference between near field and far field is the smallest. By considering a point M at the vertical of a corner of the luminaire (Fig. 1.b), we can deduce analytical expressions of the illuminance in the near-field:

$$E_\infty(\mathrm{M}) = L\int_{u=0}^{a}\int_{v=0}^{a}\frac{h^2}{\left(u^2+v^2+h^2\right)^2}dudv$$
$$= L\frac{a}{\sqrt{a^2+h^2}}\tan^{-1}\left(\frac{a}{\sqrt{a^2+h^2}}\right) \quad (9)$$

and in the far-field:

$$E_1(\mathrm{M}) = L\frac{a^2h^2}{\left(a^2/2+h^2\right)^2} \quad (10)$$

In figure 2.a, we present the relative error between the illuminance $E_1(\mathrm{M})$ calculated in far-field approximation and $E_\infty(\mathrm{M})$, calculated with the near-field assumption. For low heights *h*, the illuminance is strongly underestimated by the far-field approach before overestimating it by reaching a maximum of +6% for *h* = 0.9 m. The error then gradually decreases and tends towards 0. Indeed for $h >> a$, $E_1(M) = E_\infty(M) = L\,a^2/h^2$. The error becomes less than 1% when *h* > 3.4 m, i.e. about 4 times the largest size (diagonal) of the luminaire.

The figure 2.b shows the relative error between the calculated illuminance $E_N(\mathrm{M})$ and the illuminance calculated in near-field $E_\infty(\mathrm{M})$ for *h* = 1.6 m. The line obtained in log-log scale shows that the gain in accuracy is proportional to *N*. This is an interesting property because the value of *N* both determines the calculation time and the precision of the calculations. In the example shown here, a division of the luminaire into *N* = 4 small sources is sufficient to achieve an error less than 1% compared to 3.6% for the far field *N* = 1.

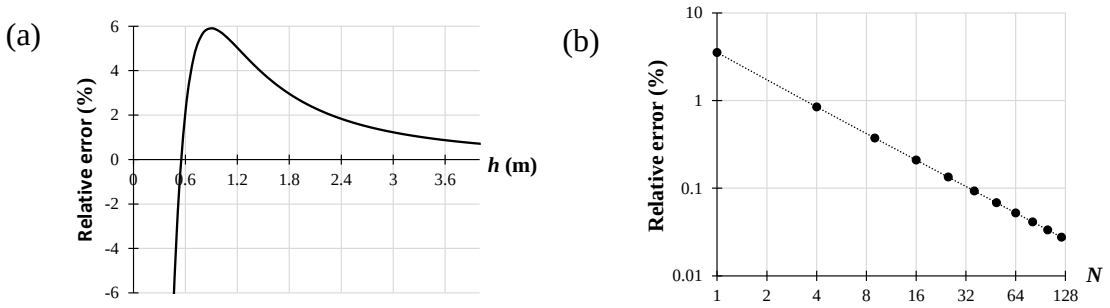

Figure 2. (a) Relative error $100(E_1 - E_\infty)/E_\infty$ as a function of the height *h*, (b) Relative error $100(E_N - E_\infty)/E_\infty$ as a function of *N* with *h* = 1.6 m (log-log scale).

3. Practical example of standard indoor lighting

Lighting configuration

In this section, we examine a typical case of standard indoor lighting. We consider a rectangular room without access to daylight. We choose the standard reflection coefficients, usually taken by default in lighting simulation software, which are 70%, 50% and 20%, respectively for the ceiling, the walls and the floor. The configuration of the room and the arrangement of the luminaires are shown in Figure 3. The ceiling and the luminaires are located at 2.4 m from the floor while the calculation surface, typically the surface of a desk, is at 0.8 m from the floor. The UGR is calculated for two positions indicated by the red and green arrows for an observer whose eyes are at 1.2 m from the ground, a realistic height for a seated person. We choose a usual room size for UGR calculations, i.e. 4*H*/8*H* with *H* being the height between the eyes of the observer and the ceiling (*H* = 1.2 m in this example). The luminaires are evenly distributed with a center-to-center distance between luminaires of *H*. However, it should be noted that this configuration is largely oversized: the average illuminance on the calculation plane is

about 3 times higher than the usual recommendations for standard rooms. This has no impact on the results since we present relative differences in illuminance values.

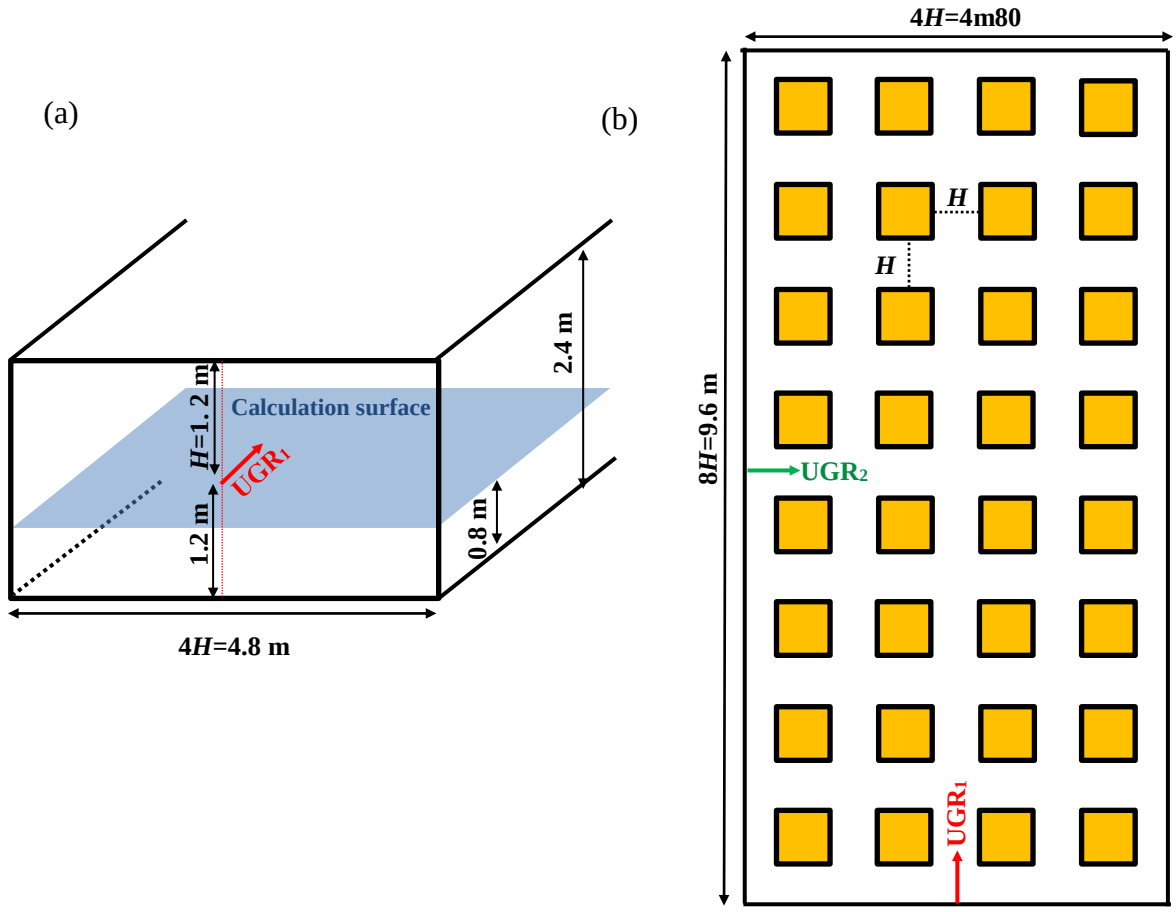

Figure 3. Room configuration, luminaire layout, illuminance calculation plane and observation positions (noted UGR_1 and UGR_2) for UGR calculations (a) 3D view, (b) Top view.

We divide the luminaire into N identical square surfaces, which are each assigned to a luminous intensity distribution. Using the Dialux 4.13 lighting simulation software, the illuminances on the calculation surface are given on a regular grid of 16 positions in width and 32 in length of the room. The illuminances E_N are compared with the illuminances E_{49}, obtained by dividing each luminaire into 7x7 small areas. UGR values calculated by the software are also recorded.

Case of a uniform luminaire

Most current LED recessed ceiling luminaires of this size incorporate a light diffuser. The luminance is assumed to be uniform over the emitting surface. We choose a commercially available LED luminaire whose luminous intensity distributions are shown in Figure 4.a. The total luminous flux is 3400 lm and the emitting surface is 0.549 x 0.549 m^2. The IES file provided by the luminaire manufacturer is modified by dividing the area of the emitting surface and each intensity value by *N*. We assign the same intensity distribution curve to the *N* point sources evenly distributed over the surface of the luminaire. The relative errors $100\left(E_N - E_{49}\right)/E_{49}$ is calculated at each point of the calculation surface. A map of these relative errors is shown in Figure 5 for $N = 1$. This map logically presents the same symmetries as the room and the lighting configuration. Relative errors are generally lower in the center of the room where indirect contributions by reflection on the walls are less important. From the values found on these maps, we calculate both the average value and the root mean square (rms) deviation , as shown in Figure 6.a in black and blue respectively. As expected, both curves decrease with *N*, emphasizing the improvement in accuracy. In this example, the average value is always positive. The decrease is much more pronounced from $N = 3\text{x}3$. The decrease of the rms deviation is more progressive and much slower. An rms deviation of less than 1% is reached only for $N = 6\text{x}6$. A division of the luminaire into 5x5 subdivisions seems to be a good trade-off, giving an average error of 0.1 % and an rms deviation of 1.3 %.

Figure 7.a shows the evolution of the UGR calculated as a function of *N* for the two configurations shown in Figure 3. As expected, the luminaire division has only a weak influence on the UGR in the case of a uniform luminaire.

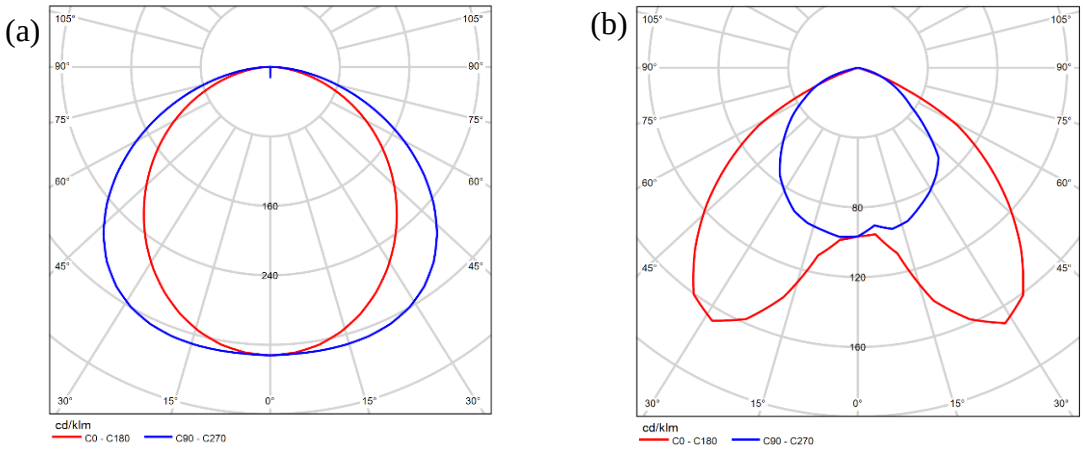

Figure 4. Intensity distribution curves (a) Case of an LED panel luminaire with uniform emission (manufacturer data), (b) Case of a T5 tube luminaire with non-uniform emission (graphs generated by the CSTB SimLuminaire software).

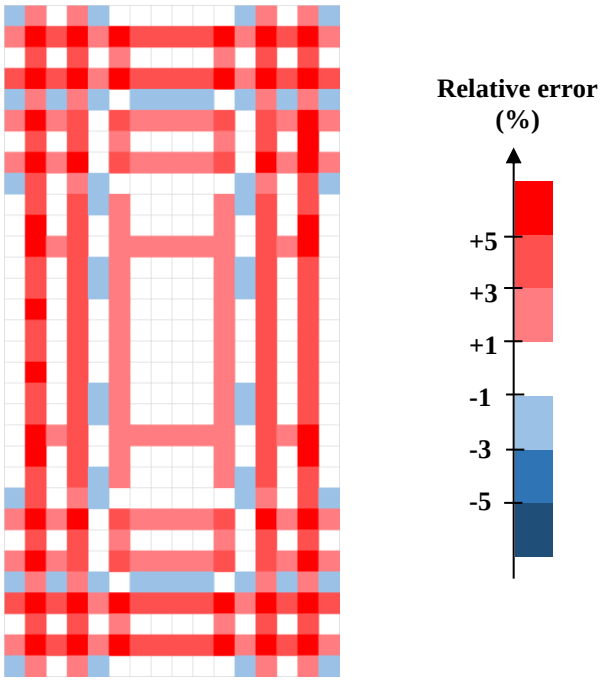

Figure 5. Map of the relative errors $100(E_1 - E_{49})/E_{49}$ for the LED panel luminaire with uniform emission.

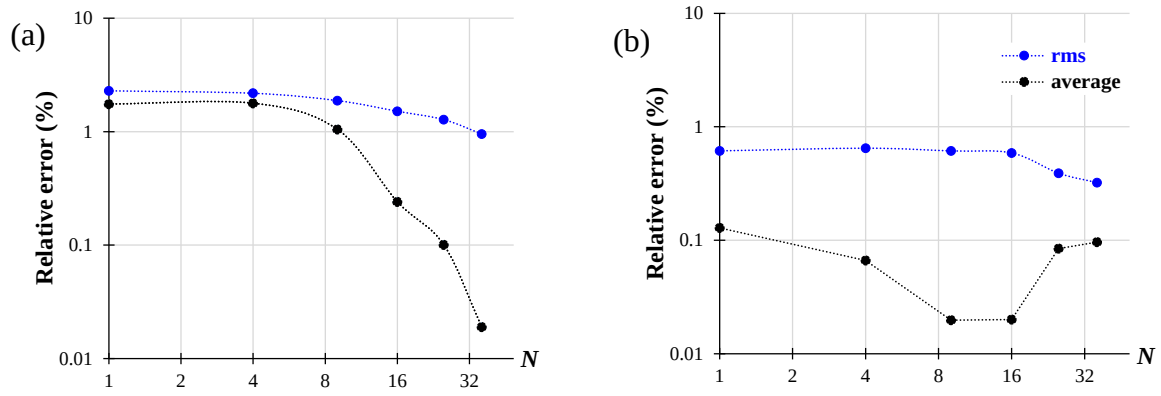

Figure 6. Average value (black curve) and root mean square deviation (blue curve) of the relative errors $100(E_N - E_{49})/E_{49}$ as a function of *N*. (a) Case of an LED luminaire with uniform emission, (b) Case of a luminaire with T5 fluorescent tubes and a non-uniform emission.

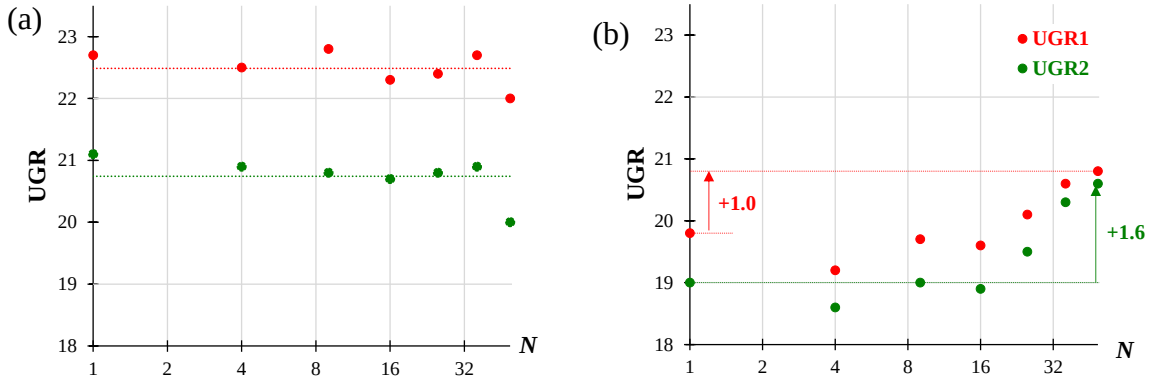

Figure 7. UGR values as a function of *N* for positions UGR_1 (in red) and UGR_2 (in green) as shown in Fig. 3.b. (a) Case of an LED panel luminaire with uniform emission, (b) Case of a luminaire with T5 fluorescent tube with non-uniform emission.

Non-uniform luminaire

We now consider a non-uniform luminaire working with T5 fluorescent tubes. To generate the intensity distribution curves, we use the CSTB SimLuminaire software, an

optical design software developed by CSTB (Carré 2017). As shown in Figure 8, the designed luminaire comprises four T5 tubes surrounded by parabolic cylindrical reflectors. It also has a scrolling grid to limit glare.

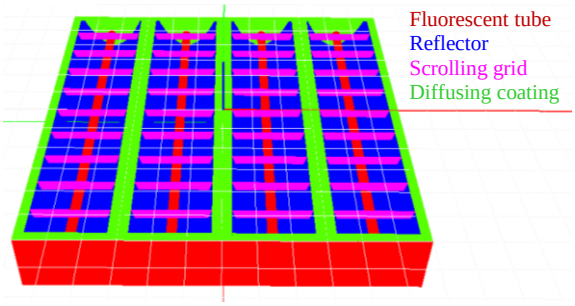

Figure 8. Luminaire with four T5 fluorescent tubes modeled by the CSTB SimLuminaire software

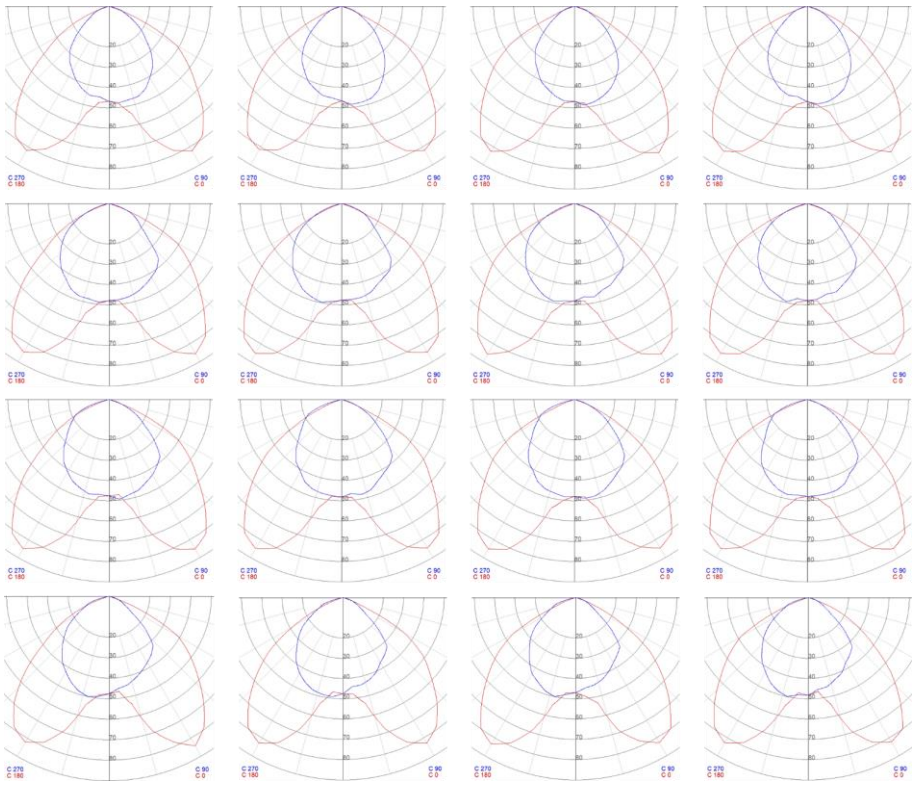

Figure 9. Intensity distribution curves generated for the 4x4 division by the CSTB SimLuminaire software

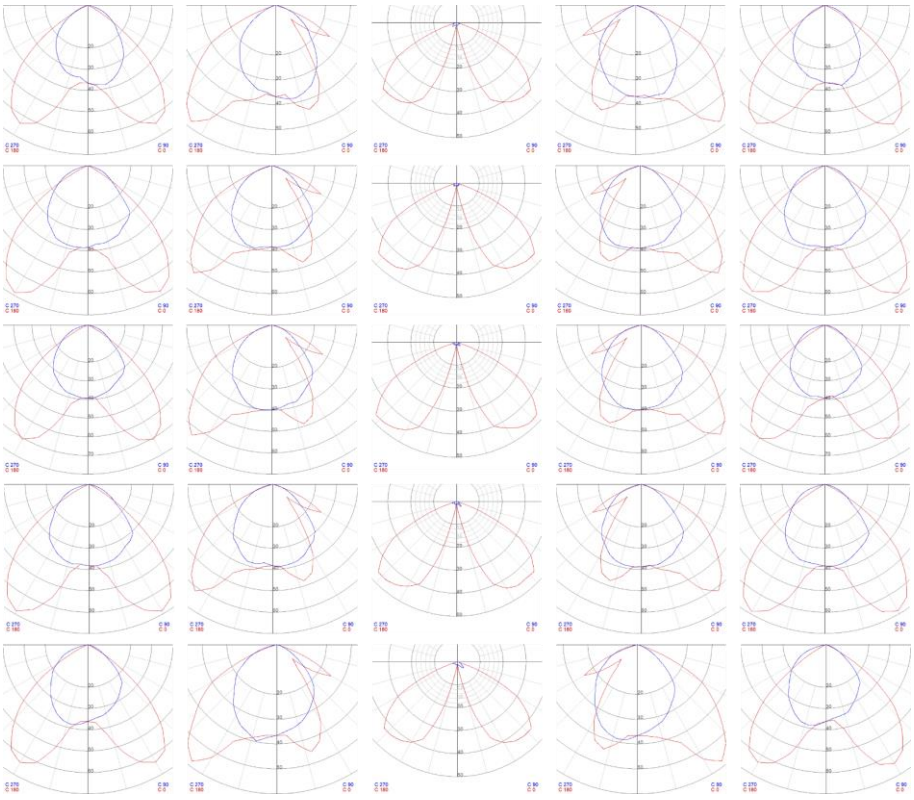

Figure 10. Intensity distribution curves generated for the 5x5 division by the CSTB SimLuminaire software.

SimLuminaire is a software based on particle tracing and ray tracing in order to take into account the multiples reflections on the luminaire surfaces. All optical phenomena (emission, absorption, scattering, reflection, transmission) are modeled in terms of probability densities. The intensity distribution curve (Fig. 4.b) is defined by considering more than 10^8 rays coming out of a previously defined virtual surface area of 0.57x0.57 m^2. This correspond to a luminous flux of 3070 lm. We can thus define *N* output surfaces to generate *N* separate IES files. In order to have comparable results, we choose a number of traced particles, and thus a simulation time, proportional to *N*. Figures 9 and 10 show the intensity distribution curves generated by SimLuminaire for 4x4 and 5x5 divisions respectively.

The average value (black curve) and the rms deviation (blue curve) for the relative errors $100(E_N - E_{49})/E_{49}$ are shown in Figure 6.b. We previously estimated that the uncertainties related to the random generation of the intensity distribution curves by SimLuminaire was about 0.2% rms. Our values of rms deviations are significantly higher than this threshold and are therefore significant. Surprisingly, these errors are small, less than 1%, even with the intensity distribution curve obtained without subdividing the luminaire. For this luminaire, the near-field approach does not bring a real improvement of the uncertainty in comparison with the far-field approach. As with the uniform luminaire (Fig. 6.a), the rms deviation decreases slightly with *N*.

The calculated UGR values are shown in Figure 7.b. Up to $N = 4\text{x}4$, these values do not change much. This can be explained by the symmetry of the luminaire. The intensity distribution curves for the 4x4 division (Fig. 9) are indeed almost identical and very close to those without division (Fig. 4.b). Due to the non-uniformity of the luminaire's emission, the UGR values increase but only from $N = 5\text{x}5$. For $N = 7\text{x}7$, the increase in UGR is +1.0 and +1.6 for positions UGR_1 and UGR_2 presented in Fig. 3, compared to the UGR calculated in the far-field configuration ($N = 1$).

4. UGR for luminaire with non-uniform emission

The CIE technical report 232:2019 defines a correction to the UGR formula (Eq. (3)) to take into account the non-uniformity of the luminance. A general expression of the corrected UGR can be written as:

$$UGR' = 8\log\frac{0.25}{L_b}\sum\frac{L_{eff}^2\,\omega_{eff}}{p^2} \qquad (11)$$

where L_{eff} is the potentially glaring effective luminance and ω_{eff} is the associated effective solid angle. A method for determining these quantities is detailed in the CIE report and consists of 4 steps.

Step1: Take high resolution luminance images

Step2: Filter images to correct for eye resolution (Gaussian filter with 12 mm FWHM at luminaire)

Step 3: Remove pixels under luminance threshold fixed at 500 cd.m^{-2}

Step 4: Calculate total area A_{eff} and average luminance L_{eff} of pixels above the luminance threshold

By entering $k^2 = L_{eff}^2 \omega_{eff} \,/\, L^2 \omega$, the equation (11) can be rewritten as follows

$$UGR' = 8\log\frac{0.25}{L_b}\sum k^2 \frac{L^2\omega}{p^2} \qquad (12)$$

Assuming that the potentially glaring "effective" parts of the luminaire are viewed from the same point and with the same obliquity factor as the actual luminaire, the ratio of solid angles $\omega_{eff} \,/\, \omega$ corresponds to the ratio of surface areas $A_{eff} \,/\, A$.

As it is very rare to have luminance images for all emission directions, the CIE technical report 232:2019 suggests to apply the same correction regardless of the configuration. Formally, the k^2-factor can be taken out of the sum of Equation (12). The correction is simply expressed as:

$$UGR' = UGR + 8\log k^2 \qquad (13)$$

The CIE technical report recommends calculating k for two azimuth angles $C = 0°$ and $C = 90°$. For each of these angles, the most penalizing (i.e. the highest) value of k for the angles $\gamma = 50°$ and $\gamma = 65°$ should be used.

The CSTB SimLuminaire software generates luminance images and consequently calculates the UGR corrections $+8\log k^2$. For the luminaire presented in Fig. 8, the corrections are +4.3 and +4.8 for positions UGR_1 and UGR_2 (red and green arrows in Fig. 3). These values are significantly higher than those obtained with the initial definition of the UGR and by splitting the luminaire into 7x7 point sources (+1.0 and +1.6, see Fig.7.b). This is because luminance values below 500 $cd.m^{-2}$ have not been discarded. The choice of the luminance threshold at 500$cd.m^{-2}$ and the consideration of two zenithal directions have a non-negligible impact in the calculated value of the corrected UGR. This impact could be assessed through psycho-visual experiments in tems of subjective notion of discomfort glare. Nevertheless, our study shows that the far-field approach underestimates the UGR in the case of a luminaire with a non-uniform emission. Therefore, near-field goniophotometry data seem to be indispensable to obtain a correct estimation of the level of discomfort glare.

5. Conclusions

Using the far-field approach, which is widely used in indoor lighting simulations, illuminances can be predicted with a deviation less than 1% of the values calculated with near-field goniophotometry data. This was demonstrated with a luminaire using four T5 fluorescent tubes, despite its non-uniformity. This counter-intuitive result may be due to the strong symmetries of the luminaire. In the case of a uniform LED panel luminaire, the errors introduced by the far-field approach are not negligible at a typical working distance from the luminaire. The results presented in this study suggest that emitting surfaces with dimensions less than 12 cm can be considered as point sources to achieve an error less than 1% in the illuminance calculations for standard indoor lighting such as office lighting. For this level of accuracy, it corresponds roughly to a ratio of 10 to the distance to the calculation plane. However, the classical "5-time rule" would in most applications

give acceptable results. We proposed to divide each luminaire into *N* smaller sources with dimensions less than 12 cm, each defined as a point source so that usual lighting simulation software can be used. For a luminaire of dimension 600 x 600 mm^2, this procedure consists in choosing a division into 5x5 equal zones. The symmetry of these luminaires would lead to only 9 different intensity distribution curves, which could be easily provided by the luminaire manufacturer. Because of these symmetries, division by an odd number (such as 5 in Fig. 10) is better able to reflect the non-uniformity than a division by an even number (such as 4 in Fig. 9). These recommendations could be generalized to other types of luminaires, such as linear luminaires with fluorescent tubes or LEDs. In this case, with the most common length of 1.2 m, a linear luminaire could be divided into 10 zones of 12 cm. Given the luminaire symmetry, five different photometric curves could be provided by the manufacturer.

For the calculation of the UGR, there is no interest in dividing the luminaire into *N* smaller areas. Indeed, when the emission is uniform, this division has no influence on the UGR. When the luminaire is non-uniform, the calculation of the UGR considering *N* point sources gives a strongly underestimated non-uniformity correction factor, compared with the calculation recommended by the CIE. With the luminance threshold arbitrarily fixed at 500 $cd.m^{-2}$ and the consideration of only two zenithal directions, the CIE non uniformity correction has the advantage of being simpler to use. However, assessing the CIE non-uniformity correction factor requires processing luminance images of the luminaire, an information, which is naturally included in a set of near-field goniophotometry data.

We believe that luminaire manufacturers should consider providing a certain amount of near-field goniophotometry data to their customers in order to improve their lighting designs with more reliable predictions of illuminance distributions and discomfort glare.

In indoor lighting, a simple procedure based on a coarse discretization of an extended luminaire only requires a small set of near-field data (typically 9 luminous intensity distributions) to significantly improve the accuracy of illuminance and UGR calculations.

Acknowledgement

We would like to thank Dr. Pierre Boulenguez for fruitful discussions on near-field photometry and for his enthusiasm, which the authors share, to promote this approach in lighting design.

Funding

The authors report no funding for the preparation of this manuscript.

Samuel Carré and Christophe Martinsons contributed to this work through the Health and Comfort Research Program SEC 2.1 of the Centre Scientifique et Technique du Bâtiment.

Disclosure statement

The authors report no declarations of interest.

References

AGI32, https://lightinganalysts.com/software-products/agi32/overview/, accessed 2021 Jan 27.

Ashdown, I. (1993). "Near-field photometry: a new approach". Journal of the Illuminating Engineering Society, 22(1), 163-180.

Ashdown, I., & Rykowski, R. (1998). "Making near-field photometry practical". Journal of the Illuminating Engineering Society, 27(1), 67-79.

Boulenguez, P., Carré, S., Piranda, B., & Perraudeau, M. (2008). "A new method of near-field photometry". J. Light Eng, 16, 89-95.

Carré S. (2017), Sim-Luminaire® Software, Centre Scientifique et Technique du Bâtiment, France

Commission Internationale de l'Eclairage (2011), Technical Report CIE 117:1995 Discomfort glare in interior lighting

Commission Internationale de l'Eclairage (2011), Technical Report CIE 198:2011 Determination of measurement incertainties in photometry

Commission Internationale de l'Eclairage (2019), Technical Report CIE 232:2019 Discomfort Caused by Glare from Luminaires with a Non-Uniform Source Luminance

DIALux evo, https://www.dialux.com/en-GB/download, accessed 2021 Jan 27.

DiLaura, D. L., Houser, K., Mistrick, R., & Steffy, G. R. (2011). "The lighting handbook: reference and application". 10th edition. Illuminating Engineering Society.

Holmes, J. G. (1990). "Photometry from the right distance". Lighting Research & Technology, 22(4), 183-187.

Lautzenheiser, T., Weller, G., & Stannard, S. (1984). "Photometry for near field applications". Journal of the Illuminating Engineering Society, 13(2), 262-269.

Ngai, P. Y. (1987). "On near-field photometry". Journal of the Illuminating Engineering Society, 16(2), 129-136.

Ngai, P. Y., Zhang, J. X., & Quan, Y. (1993). "On computation using far-field and near-field photometry". Journal of the Illuminating Engineering Society, 22(2), 118-149.

ReluxDesktop, https://relux.com/en/relux-desktop.html, accessed 2021 Jan 27.

Stannard, S., & Brass, J. (1990). "Application distance photometry". Journal of the Illuminating Engineering Society, 19(1), 39-46.